

Square-Planar Coordinated Polyanions of Palladium, Platinum, and Gold Stannaborate $[\text{SnB}_{11}\text{H}_{11}]^{2-}$ Coordination Chemistry

Thiemo Marx,^[a] Bernd Mosel,^[b] Ingo Pantenburg,^[a] Siegbert Hagen,^[a] Herbert Schulze,^[a] and Lars Wesemann*^[a]

Abstract: The tetrasubstituted polyanions of platinum, palladium, and gold $[\text{M}(\text{SnB}_{11}\text{H}_{11})_4]^{x-}$ ($x = 6$, $\text{M} = \text{Pd}$, Pt ; $x = 5$, $\text{M} = \text{Au}$) have been prepared and characterized by single-crystal X-ray diffraction, elemental analysis, IR, Raman, ^{11}B , and ^{119}Sn heteronuclear NMR spectroscopy. In the case of the platinum

derivative $[\text{Bu}_3\text{MeN}]_6[\text{Pt}(\text{SnB}_{11}\text{H}_{11})_4]$ (**2**) ^{119}Sn Mössbauer spectroscopy has been carried out. The isolated salts are stable

towards moisture and air and the complexes **2** and **3** were treated with 1,3-bis(diphenylphosphino)propane (dppp) to give the respective substitution products $[\text{Bu}_3\text{MeN}]_2[(\text{dppp})\text{M}(\text{SnB}_{11}\text{H}_{11})_2]$ ($\text{M} = \text{Pd}$, Pt).

Keywords: boranes • cluster compounds • gold • Mössbauer spectroscopy • platinum • palladium

Introduction

For more than thirty years the coordination chemistry of tin has been an active field of research.^[1] Formation of bonds between tin and transition-metals is of particular interest in the field of heterometallic cluster synthesis as well as in homogeneous catalysis since the $[\text{SnCl}_3]^-$ ligand is a prominent cocatalyst.^[1–4] In recent years bis(amino)stannylenes $[\text{Me}_2\text{Si}(\text{N}t\text{Bu})_2\text{Sn}]$,^[5] dialkylstannylenes $[\text{Sn}\{\text{CH}(\text{SiMe}_3)_2\}_2]$,^[6] and triamidostannates $[\text{MeSi}\{\text{SiMe}_2\text{N}(4\text{-CH}_3\text{C}_6\text{H}_4)\}_3\text{Sn}]^-$ and $[\text{H}_3\text{CC}(\text{CH}_2\text{NSiMe}_3)_3\text{Sn}]^{-[7]}$ have been proven to be versatile ligands in transition-metal chemistry. We have recently started an exploration of the coordination chemistry of a tin-containing *closo*-heteroborate. The preparation of the cluster $[\text{SnB}_{11}\text{H}_{11}]^{2-}$ is achieved easily by following a procedure developed by Todd and co-workers.^[8] Thus, stanna-*closo*-dodecaborate can be synthesized with different counterions offering the possibility of dissolving the ligand salt either in water or dichloromethane. By coordinating the anionic tin ligand with cationic electrophiles, zwitterionic molecules were systematically constructed.^[9] It turned out that the cluster $[\text{SnB}_{11}\text{H}_{11}]^{2-}$ exhibits a strong *trans* influence and lability in coordination at square-planar coordinated platinum(II) centers. Interestingly, this heteroborate activates aryl–platinum

complexes towards isonitrile insertion and hydroformylation.^[10, 11]

Homoleptic complexes with tin ligands are known for the trichlorostannyl $[\text{Pt}(\text{SnCl}_3)_3]^{3-}$ ^[12] and bis(amino)stannylenes $[\text{Pt}\{\text{Sn}(\text{N}t\text{Bu})_2\text{SiMe}_2\}_4\text{Cl}_2]$.^[5] To synthesize the first homoleptic derivatives with stanna-*closo*-dodecaborate as the ligand, the reactions with platinum, palladium and gold halides were investigated.

Here we present the tetrasubstitution at palladium(II), platinum(II), and gold(III) centers resulting in the isolation of nearly square-planar coordinated polyanions.

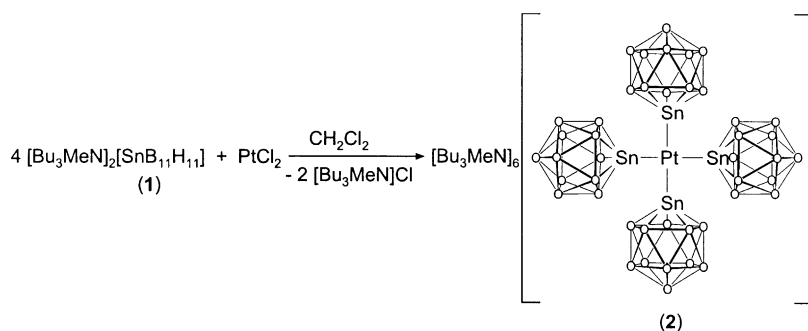
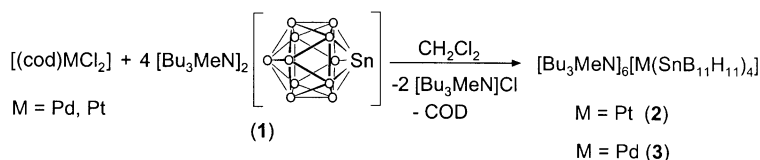
Results and discussion

Syntheses: Four equivalents of the heteroborate **1** were reacted at room temperature with a suspension of PtCl_2 in dichloromethane. Immediately the color of the reaction mixture changed to orange. Evidence that the reaction had proceeded to completion was provided by ^{11}B NMR spectroscopy (Scheme 1).

The course of the reaction could easily be monitored by ^{11}B NMR spectroscopy: the uncoordinated heteroborate shows resonances around $\delta = -11$ and -13 ppm, whereas, due to isochromism, the $\text{M-SnB}_{11}\text{H}_{11}$ unit exhibits a single signal at $\delta = -16$ ppm for ten boron atoms (the signal for B12 could not be detected). Yellow crystals of the platinum salt **2** were obtained after washing with water and crystallization from dichloromethane. From reaction with $[(\text{cod})\text{PtCl}_2]$ ($\text{cod} = 1,5$ -cyclooctadiene) the tetrasubstituted product **2** was also isolated in excellent yield. In accordance with this procedure the homologous palladium complex **3** was synthesized in yields around 90% starting from $[(\text{cod})\text{PdCl}_2]$ (Scheme 2).

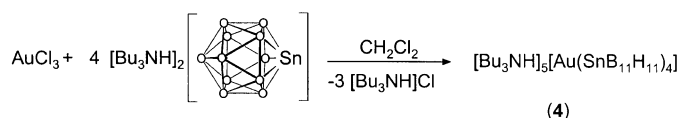
[a] Prof. Dr. L. Wesemann, T. Marx, I. Pantenburg, S. Hagen, H. Schulze
Institut für Anorganische Chemie
Universität zu Köln, Greinstrasse 6, 50939 Köln (Germany)
Fax. (+49) 221-470-5083
E-mail: lars.wesemann@uni-koeln.de

[b] B. Mosel
Institut für Physikalische Chemie
Universität Münster, Schlossplatz 4/7, 48149 Münster (Germany)

Scheme 1. Synthesis of the tetrasubstituted platinum complex **2**.Scheme 2. Reaction of $[(\text{cod})\text{MCl}_2]$ (M = Pd, Pt) with stanna-*closo*-dodecaborate **1** (cod = 1,5-cyclooctadiene).

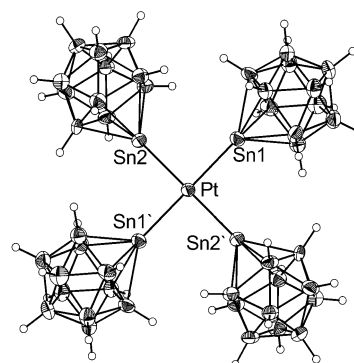
The hexaanions **2** and **3** are resistant towards moisture and air and show no reaction with further equivalents of stanna-borate ligand **1**. However, in contrast to this reaction is the pentacoordination in $[\text{Pt}(\text{SnCl}_3)_5]^{3-}$. The substitution of the cyclooctadienyl ligand (Scheme 2) is surprising since the comparable trichlorostannyl ligand shows no tendency to displace the diolefin. The trichlorostannyl substituted olefin complexes $[\text{N}(\text{PPh}_3)_2][\text{M}(\text{SnCl}_3)_3(\text{cod})]$ (M = Pd, Pt) are known from the literature.^[13] These findings might be interpreted as a further indicator for the stronger *trans*-influence of the heteroborate ligand **1** in comparison to the trichlorostannyl ligand in the chemistry of platinum(II) and palladium(II).

Red-orange crystals of the tetrasubstitution product $[\text{Bu}_3\text{N-H}]_5[\text{Au}(\text{SnB}_{11}\text{H}_{11})_4]$ (**4**) were obtained from the reaction of gold(III) chloride with cluster nucleophile (Scheme 3). The coordination chemistry of tin with gold is much less developed and the corresponding homoleptic trichlorostannyl complex is so far unknown.^[7, 14, 15, 16]

Scheme 3. Formation of the tetrasubstituted Au^{III} complex **4**.

Solid-state structure: Crystallization of the tetraalkylammonium derivatives **2** and **3** resulted in the isolation of yellow crystals suitable for single-crystal structure analysis. The $[\text{Bu}_3\text{MeN}]_6[\text{Pt}(\text{SnB}_{11}\text{H}_{11})_4]$ (**2**) salt crystallizes in the triclinic space group $P\bar{1}$ under the inclusion of two equivalents of dichloromethane. The structure of the

hexaanion in the solid state is depicted in Figure 1 and the data of the structure solution and refinement are listed in Table 1. However, due to tetraalkylammonium disorder in the solid state the counteranions were refined without hydrogen atoms. The square-planar coordination around the platinum center is nearly ideal; the transition metal is situated at the center of symmetry. The interatomic separations of Pt–Sn1 2.554(1), Pt–Sn2 2.565(1) Å, and Sn–B 2.314(8)–2.347(8) are in the range of those of other stanna-*closo*-dodecaborate complexes of platinum.^[9] The analogous palladium salt crystallizes in the same space group but the disorder problems are even worse and therefore a suitable structure solution was not obtained.

Figure 1. Molecular structure of the $[\text{Pt}(\text{SnB}_{11}\text{H}_{11})_4]^{6-}$ ion of **2** in the solid state; the hexaanion lies on a center of symmetry. Interatomic distances [Å] and angles [°]: Pt–Sn1 2.554(1), Pt–Sn2 2.565(1); Sn1–Pt–Sn2 91.18(2).

To overcome the crystallographic problems of the tetraalkylammonium disorder we decided to change the counteranions from alkylammonium to potassium/crown ether. The tetracoordinate platinum and palladium complexes were isolated as the $[\text{Bu}_3\text{NH}]$ salts **5** and **7** and then allowed to react with six equivalents of hydride $\text{K}[\text{HBEt}_3]$ (Scheme 4).

Crystallization was carried out after addition of crown ether from acetonitrile or a mixture of THF and acetone. $[\text{K}(18\text{-crown-6})]_6[\text{Pt}(\text{SnB}_{11}\text{H}_{11})_4]$ (**6**) crystallizes with the inclusion of four molecules of acetone and two molecules of water as pale

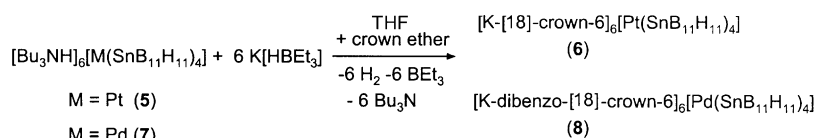
Scheme 4. Exchange of the counteranion $[\text{Bu}_3\text{NH}]^+$ with potassium.

Table 1. Crystal data and structure refinement parameters for **2**, **4**, **6**, and **10**.

	2	4	6	10
empirical formula	C ₈₂ H ₂₃₂ B ₄₄ N ₆ Cl ₈ Sn ₄ Pt	C ₆₀ H ₁₈₄ B ₄₄ N ₅ Sn ₄ Au	C ₈₄ H ₂₁₆ B ₄₄ O ₄₂ K ₆ Sn ₄ Pt	C ₅₃ H ₁₀₈ B ₂₂ N ₂ P ₂ Sn ₂ Pd
formula mass	2731.83	2123.49	3278.66	1416.95
<i>data collection</i>				
diffractometer	STOE IPDS II	STOE IPDS II	STOE IPDS I	STOE IPDS II
radiation		MoK α (graphite monochromator, $\lambda = 71.073$ pm)		
temperature [K]	170(2)	170(2)	170(2)	170(2)
index range	$-15 \geq h \geq 15$ $-19 \geq k \geq 21$ $-22 \geq l \geq 22$	$-17 \geq h \geq 17$ $-19 \geq k \geq 19$ $-20 \geq l \geq 20$	$-25 \geq h \geq 25$ $-29 \geq k \geq 29$ $-26 \geq l \geq 26$	$-22 \geq h \geq 22$ $-25 \geq k \geq 25$ $-25 \geq l \geq 26$
rotation angle range	$0^\circ \geq \omega \geq 180^\circ$; $\psi = 0^\circ$ $0^\circ \geq \omega \geq 180^\circ$; $\psi = 90^\circ$	$0^\circ \geq \omega \geq 180^\circ$; $\psi = 0^\circ$ $0^\circ \geq \omega \geq 180^\circ$; $\psi = 90^\circ$	$0^\circ \geq \psi \geq 250^\circ$	$0^\circ \geq \omega \geq 180^\circ$; $\psi = 0^\circ$ $0^\circ \geq \omega \geq 180^\circ$; $\psi = 90^\circ$ $0^\circ \geq \omega \geq 20^\circ$; $\psi = 135^\circ$
increment	$\Delta\omega = 2^\circ$	$\Delta\omega = 2^\circ$	$\Delta\psi = 2^\circ$	$\Delta\omega = 2^\circ$
no. of images	180	180	125	190
exposure time [min]	2	4	5	2
detector distance [mm]	120	80	60	120
2θ range [°]	1.9–54.8	2.9–64.8	3.8–56.3	1.9–54.8
total data collected	43 746	46 235	68 060	106 127
unique data	13 569	13 023	15 323	8085
observed data	8749	7858	8592	4474
R_{merg}	0.0536	0.0866	0.1142	0.1490
absorption correction		numerical, after crystal shape optimization ^[17, 18]		
transmission min/max	0.6586/0.8094	0.6366/0.8072	0.7142/0.8441	0.4949/0.7655
<i>crystallographic data</i> ^[19]				
crystal size [mm]	0.3 × 0.3 × 0.2	0.2 × 0.2 × 0.1	0.25 × 0.25 × 0.2	0.3 × 0.3 × 0.2
color, habit	yellow, column	colorless, polyhedron	colorless, column	yellow, polyhedron
crystal system	triclinic	triclinic	monoclinic	orthorhombic
space group	$P\bar{1}$ (no. 2)	$P\bar{1}$ (no. 2)	$P2_1/m$ (no. 11)	$Pnab$ (no. 60)
a [pm]	1199.1(1)	1437.1(2)	1923.6(3)	1794.2(1)
b [pm]	1703.0(2)	1566.6(1)	2238.3(3)	1966.8(1)
c [pm]	1746.8(2)	1697.6(2)	2024.5(3)	2035.6(2)
α [°]	83.83(1)	116.86(2)		
β [°]	89.28(1)	100.17(1)	95.61(2)	
γ [°]	79.67(1)	93.41(1)		
volume [nm ³]	3.4887(5)	3.3138(6)	8.6749(22)	7.1831(10)
Z	1	1	2	4
ρ_{calcd} [g cm ⁻³]	1.300	1.064	1.255	1.310
μ [mm ⁻¹]	1.896	1.875	1.575	1.017
$F(000)$	1400	1078	3336	2904
<i>structure analysis and refinement</i>				
structure determination		SHELXS-97 ^[20] and SHELXL-93 ^[21]		
no. of variables	451	461	837	373
R indexes ^[a] [$I > 2\sigma I$]				
R_1	0.0567	0.0688	0.0588	0.0535
wR_2	0.1431	0.1999	0.1653	0.1253
R indexes (all data)				
R_1	0.0858	0.1107	0.1137	0.0952
wR_2	0.1509	0.2217	0.1896	0.1362
goodness of fit (S_{obs})	1.105	0.960	1.107	1.127
goodness of fit (S_{all})	0.931	0.960	0.932	0.897
largest difference map hole/peak [$e \cdot 10^{-6} \text{ pm}^{-3}$]	-1.537/1.925	-0.762/2.305	-1.194/3.683	-0.825/1.107

[a] $R_1 = \sum (|F_o| - |F_c|) / \sum |F_o|$, $wR_2 = [\sum w (|F_o|^2 - |F_c|^2)^2 / \sum w |F_o|^2]^{1/2}$, $S_2 = [\sum w (|F_o|^2 - |F_c|^2)^2 / (n - p)]^{1/2}$, with $w = 1/[\sigma^2(F_o)^2 + (0.0908P)^2]$ for **2**, $w = 1/[\sigma^2(F_o)^2 + 0.1375P^2]$ for **4**, $w = 1/[\sigma^2(F_o)^2 + (0.1095P)^2]$ for **6** and $w = 1/[\sigma^2(F_o)^2 + (0.0741P)^2]$ for **10**, were $P = (F_o^2 + 2F_c^2)/3$. $F_c^* = kF_c [1 + 0.001 \times |F_c|^2 \lambda^3 / \sin(2\theta)]^{-1/4}$.

yellow rods in the monoclinic space group $P2_1/m$. The platinum atom and two tin atoms lie on the mirror plane and the platinum center is almost square-planar coordinated by four heteroborate ligands. The deviation of 11° from 180° for the Sn-Pt-Sn angle can be interpreted as an indication for a slight distortion of the square-planar coordination towards a tetrahedral geometry. Three of the six countercations are coordinated at the cluster sphere, each by means of three

K-H-B-bonds, whereas the other cations exhibit coordination with additional acetone or water molecules. Figure 2 shows the hexaanion and the coordinated potassium cations without the crown ether molecules. Data for the structure solution and refinement are listed in Table 1.

Interestingly, the hexaanions $[\text{Pt}(\text{SnB}_{11}\text{H}_{11})_4]^{6-}$ are packed in stacks in the structures of **2** and **6** with different countercations. In the case of the $[\text{Bu}_3\text{MeN}]$ cation these stacks are

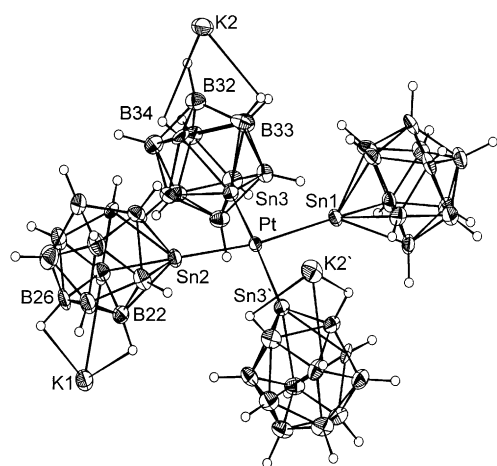


Figure 2. Structure of **6** in the solid state. Potassium cations without coordination at the cluster sphere and the crown ether molecules have been omitted for clarity. The atoms Pt, Sn1, Sn2, K1, and B26 lie on a mirror plane. Interatomic distances [Å] and angles [°]: Pt–Sn1 2.559(1), Pt–Sn2 2.563(1), Pt–Sn3 2.570(1), K1–B22 3.35(1), K1–B26 3.32(2), K2–B32 3.39(1), K2–B34 3.33(1), K2–B33 3.33(1); Sn1–Pt–Sn2 169.14(3), Sn1–Pt–Sn3 90.14(2), Sn2–Pt–Sn3 90.85(2), Sn3–Pt–Sn3' 169.49(3).

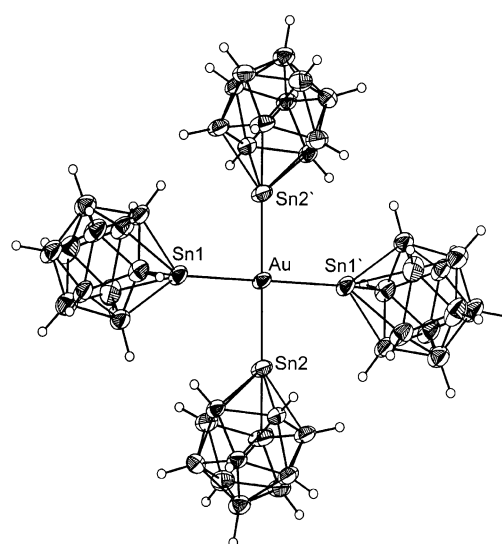


Figure 3. Molecular structure of the anion of **4** in the solid state; the pentaanion lies on a center of symmetry. Interatomic distances [Å] and angles [°]: Au–Sn1 2.601(1), Au–Sn2 2.589(1); Sn1–Au–Sn2 90.42(2), Sn1–Au–Sn2' 89.58(2).

arranged along the *a* axis with a Pt–Pt separation of 11.99 Å, whereas in the structure of **6** they are arranged along the *c* axis with a Pt–Pt separation of 20.25 Å.

The palladium salt **8** was crystallized with dibenzocrown ether as the chelating ligand. Yellow crystals of this salt were obtained from acetonitrile at 0°C. Unfortunately these crystals were not suitable for single-crystal structure analysis. To study the anion packing in the solid-state and its dependency on the charge of the counteranion we tried to crystallize dications with the hexaanions. The salt $[\text{py}-(\text{CH}_2)_4\text{-py}]_3[\text{Pt}(\text{SnB}_{11}\text{H}_{11})_4]^{6-}$ was obtained as a red, analytically pure substance but due to the very low solubility even in polar solvents like DMSO we were not able to recrystallize this salt.

Crystals of the tetracoordinate gold derivative $[\text{Au}(\text{SnB}_{11}\text{H}_{11})_4]^{5-}$ were obtained with the $[\text{Bu}_3\text{NH}]^+$ ion. The salt crystallizes in the triclinic space group $P\bar{1}$ with the gold atom at the center of symmetry. The boron, gold, and tin atoms of the pentaanion were refined anisotropically and the hydrogen atoms connected to the boron atoms were placed in calculated positions. Two cations were found in the asymmetric unit and the respective carbon and nitrogen atoms were refined anisotropically. Electron density peaks for the remaining half cation were found in the difference Fourier map but we were not able to solve the disorder of the Bu_3NH cation with respect to the inversion center. The structure of the pentaanion in the solid state is depicted in Figure 3 and the data for the structure solution and refinement are listed in Table 1. The Au–Sn interatomic separation (2.589(1), 2.601(1) Å) is only slightly longer than that in $[\text{MeSi}(\text{SiMe}_2\text{N}(4\text{-CH}_3\text{C}_6\text{H}_4))_3\text{Sn}-\text{Au}(\text{PPh}_3)]$ (2.565(1) Å).^[7b]

Spectroscopic characterization: To further characterize the tin–metal complexes and to obtain information about the electronic environment of the tin atom, ^{119}Sn NMR and ^{119}Sn Mössbauer spectroscopy were carried out on the platinum complex **2**. The ^{119}Sn NMR and Mössbauer spectroscopy data of the uncoordinated ligand **1**, the platinum derivative **2** and the methylsubstituted stannaborate $[\text{MeSnB}_{11}\text{H}_{11}]^-$ are listed in Table 2.^[8] The NMR spectroscopic data depend strongly on the oxidation state of the tin atom; however, the determination of the absolute valence state from the NMR chemical shift is very difficult.^[22] Several factors contribute to the shielding of a nucleus in a molecular environment. In the presented series of anions $[\text{SnB}_{11}\text{H}_{11}]^{2-}$, $[\text{Pt}(\text{SnB}_{11}\text{H}_{11})_4]^{6-}$, and $[\text{MeSnB}_{11}\text{H}_{11}]^-$ the ^{119}Sn chemical shift rises from $\delta = -546$ to -197 ppm. These spectroscopic findings are consistent with the formal oxidation states of the tin nucleus of Sn^{II} and Sn^{IV} in **1** and $[\text{MeSnB}_{11}\text{H}_{11}]^-$, respectively.

Most organometallic tin compounds show ^{119}Sn Mössbauer isomer shifts in the range from 0–4 mms^{-1} relative to CaSnO_3 , and the value for α -tin (2.05 mms^{-1}) is often regarded as the borderline between the formal oxidation states Sn^{II} (> 2.05 mms^{-1}) and Sn^{IV} (< 2.05 mms^{-1}).^[23, 24] Thus, in the presented series $[\text{SnB}_{11}\text{H}_{11}]^{2-}$ (IS = 2.46 mms^{-1}), $[\text{Pt}(\text{SnB}_{11}\text{H}_{11})_4]^{6-}$ (IS = 1.66 mms^{-1}), (Figure 4) and $[\text{MeSn}$

Table 2. ^{119}Sn Mössbauer and NMR spectroscopy for **1**, **2**, and $[\text{Ph}_3\text{MeP}][\text{MeSnB}_{11}\text{H}_{11}]^{8]}$

	^{119}Sn Mössbauer data [mms^{-1}]		^{119}Sn NMR chemical shift [ppm]
	IS	EFG	
$[\text{Bu}_3\text{MeN}]_2[\text{SnB}_{11}\text{H}_{11}]^{[a]}$ (1)	2.46	1.71	–546
$[\text{Bu}_3\text{MeN}]_6[\text{Pt}(\text{SnB}_{11}\text{H}_{11})_4]$ (2)	1.66	1.51	–317 ($J_{\text{Pt,Sn}} = 14000$ Hz)
$[\text{Ph}_3\text{MeP}][\text{MeSnB}_{11}\text{H}_{11}]$	1.18	0.95	–97

[a] The Mössbauer spectrum of **1** shows a further signal (IS = 1.74 mms^{-1} ; EFG = 2.7 mms^{-1}) even after repeated recrystallization of the salt **1** and in different matrices.

$B_{11}H_{11}]^{-}$ (IS = 1.18 mms^{-1}), the isomer shift varies from Sn^{II} to Sn^{IV} and confirms the ^{119}Sn NMR spectroscopic data. Since the s orbitals are the only orbitals with appreciable electron density at the nucleus, an decreasing IS value ($[\text{SnB}_{11}\text{H}_{11}]^{2-}$ IS = 2.47 mms^{-1} , $[\text{Pt}(\text{SnB}_{11}\text{H}_{11})_4]^{6-}$ IS = 1.66 mms^{-1}) can be interpreted as an indicator of donation of electron density from the tin atom to the platinum center.^[1a, 1b]

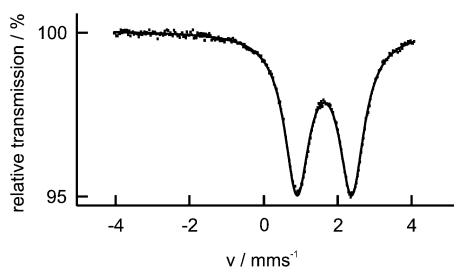
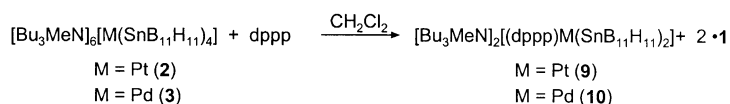


Figure 4. Experimental and simulated ^{119}Sn Mössbauer spectrum of $[\text{Bu}_3\text{MeN}]_6[\text{Pt}(\text{SnB}_{11}\text{H}_{11})_4]$ (**2**) recorded at 78 K.

From the IR and Raman spectroscopic measurements the Pd–Sn and Pt–Sn stretching frequencies in the square planar coordinated hexaanions could be determined. As expected, the values for the Pt–Sn vibration occur at lower energy (170 cm^{-1}) in comparison to the Pd–Sn vibration (191 cm^{-1}). In the case of the gold derivative **4** a resonance for the Au–Sn vibration (159 cm^{-1}) was observed only in the IR spectra.^[1b]

As listed in Table 2, the ^{119}Sn resonance for the platinum derivative **2** appears at $\delta = -317$ ppm with a $^1J(^{119}\text{Sn}, ^{195}\text{Pt})$ coupling constant of 14000 Hz. For square-planar tin–platinum complexes the tin–platinum coupling constant is strongly dependent on the nature of the ligand *trans* to the tin atom.^[1b] Ligands with a weak *trans* influence, like chloride, result in the observation of $^1J(^{119}\text{Sn}, ^{195}\text{Pt})$ coupling constants around 26000–35300 Hz.^[25] In contrast, the hydride ligand, with a very strong *trans* influence, weakens the Pt–Sn bond, and as a consequence the coupling constants are much smaller (9000–11500 Hz).^[1b] In the presented example a stannaborate ligand is always *trans* to the Pt–Sn unit and this ligand is therefore responsible for the coupling constant of 14000 Hz, whereas the trichlorostannyl ligand $[\text{SnCl}_3]^{-}$ causes coupling constants of around 19000–24000 Hz. This might be interpreted as a further indicator for the already published stronger *trans* influence of the heteroborate **1** in comparison to the $[\text{SnCl}_3]^{-}$ group.^[9b]

Reactivity: In the case of the trichlorostannyl ligand a five-coordinate platinum complex $[\text{Pt}(\text{SnCl}_3)_5]^{3-}$ is known from the literature. We found no indication of a coordination number higher than four in reactions of the hexaanions of palladium and platinum and the pentaanion of gold with excess stannaborate. Two of the stannaborate ligands could be replaced upon reaction with chelating phosphines like 1,3-bis(diphenylphosphino)propane (dppp) (Scheme 5). The synthesis of the platinum complex **9** starting from the $[(\text{dppp})\text{PtCl}_2]$ dichloride has already been published and the hydroformylation activity of the dianion **9** investigated.^[11] The



Scheme 5. Reaction of the tetrasubstituted palladium and platinum complexes with a chelating phosphine (dppp = 1,3-bis(diphenylphosphino)propane).

dianions of the type $[(\text{dppp})\text{M}(\text{SnB}_{11}\text{H}_{11})_2]^{2-}$ were characterized by NMR spectroscopy and, in the case of the so-far-unknown palladium complex **10**, by single-crystal X-ray diffraction. Data for the X-ray crystal structure measurement are listed in Table 1 and Figure 5 shows an Ortep plot of the

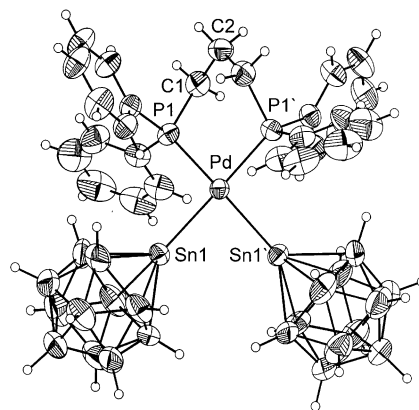


Figure 5. Molecular structure of the anion of **10** in the solid state; the dianion lies on a twofold rotation axis. Interatomic distances [Å] and angles [°]: Pd–Sn1 2.578(1), Pd–P1 2.313(1), P1–C1 1.830(6), C1–C2 1.535(7); P1–Pd–Sn1' 167.61(3), P1–Pd–Sn1 91.85(4), P1–Pd–P1' 91.42(7), Sn1–Pd–Sn1' 87.49(2).

dianion of **10** in the solid state. Both the platinum and palladium salt crystallize in the orthorhombic space group $Pbcn$ with nearly identical cell dimensions. The cell of the palladium derivative is 1.7% larger than the cell of the homologous platinum complex. The transition-metal complex **10** lies on a twofold rotation axis and, due to steric crowding around the metal center, the square-planar configuration is slightly distorted towards a tetrahedral arrangement (torsion angle: $\text{P–P'–Sn–Sn}' = 25^\circ$).

Conclusion

Four stanna-*closo*-dodecaborate clusters coordinate in a square-planar coordination mode at the d^8 -transition-metal centers Pd^{II} , Pt^{II} , and Au^{III} . The tin-polyborate ligand is a strong enough nucleophile to displace the COD ligand in the respective palladium and platinum complexes $[(\text{cod})\text{MCl}_2]$.

Experimental Section

All manipulations were carried out under dry N_2 in Schlenk glassware; solvents were dried and purified by standard methods and were stored under N_2 ; NMR Bruker AC 200 (^1H : 200 MHz, int. TMS; $^{31}\text{P}\{^1\text{H}\}$: 81 MHz, ext. 85% H_3PO_4 ; $^{11}\text{B}\{^1\text{H}\}$: 64 MHz, ext. $\text{BF}_3 \cdot \text{Et}_2\text{O}$) NMR Bruker AC 300 (^{119}Sn : 112 MHz, ext. SnMe_4); elemental analysis: Institut für Anorganische

Chemie der Universität zu Köln, Heraeus C,H,N,O-Rapid elemental analyser; IR/Raman spectrometer: IFS66v/s Bruker. ^{119}Sn Mössbauer spectra were recorded by using a linear arrangement of source, absorber and NaI(Tl) scintillation detector. Sn absorbers were cooled to 78 K using a bath cryostat (MD 300, Oxford). The source $\text{Ca}^{119\text{m}}\text{SnO}_3$ (Wissel) was kept at room temperature. The velocity scale is calibrated by a laser interferometer. The experimental data were fitted to Mössbauer sites with isomer shift IS and electrical field gradient EFG.

[Bu₃MeN]₆[Pt(SnB₁₁H₁₁)₄] (2): $[\text{Bu}_3\text{MeN}]_2[\text{SnB}_{11}\text{H}_{11}]$ (**1**) (1.20 g, 1.85 mmol) was dissolved in CH_2Cl_2 (20 mL) and treated with a solution of $[(\text{cod})\text{PtCl}_2]$ (0.17 g, 0.45 mmol) in CH_2Cl_2 (20 mL) at room temperature. After the mixture was stirred overnight, the solvent was evaporated and the residue was dissolved in acetone (40 mL). Then an aqueous saturated NaCl solution (40 mL) was slowly added. The yellow precipitate was isolated by filtration and dried under vacuum. Yield: 1.00 g, 92%. Recrystallization was carried out in CH_2Cl_2 by slow diffusion of hexane at 0 °C to give crystals of **2**. $^{11}\text{B}\{^1\text{H}\}$ NMR (64 MHz, $[\text{D}_6]\text{acetone}$, 25 °C): $\delta = -15.9$ ppm (br; B2–B11), signal for B12 not detected; ^{119}Sn NMR (112 MHz, CD_2Cl_2 , 25 °C): $\delta = -317$ ppm (br, $^1J_{\text{Pt,Sn}} = 14000$ Hz); elemental analysis calcd (%) for $\text{PtSn}_4\text{B}_{44}\text{N}_6\text{C}_{78}\text{H}_{224}$ (2392.18): C 39.16, H 9.44, N 3.51; found: C 38.89, H 9.36, N 3.56.

Instead of reacting a solution of $[(\text{cod})\text{PtCl}_2]$ in CH_2Cl_2 , a suspension of PtCl_2 in the same solvent can be used (yield: 81% of **2**).

[Bu₃MeN]₆[Pd(SnB₁₁H₁₁)₄] (3): Compound **1** (1.00 g, 1.54 mmol) was dissolved in CH_2Cl_2 (20 mL) and treated with a solution of $[(\text{cod})\text{PdCl}_2]$ (0.11 g, 0.39 mmol) in CH_2Cl_2 (20 mL) at room temperature. After the mixture was stirred overnight, the solvent was evaporated and the residue was dissolved in acetone (40 mL). An aqueous saturated NaCl solution (40 mL) was slowly added. The yellow precipitate was isolated by filtration and dried under vacuum. Yield: 0.70 g, 78%. Recrystallization was carried out in CH_2Cl_2 by slow diffusion of hexane at 0 °C to give yellow crystals of **3**. $^{11}\text{B}\{^1\text{H}\}$ NMR (64 MHz, CD_2Cl_2 , 25 °C): $\delta = -6.0$ (B12), -15.1 ppm (B2–B11); elemental analysis calcd (%) for $\text{PdSn}_4\text{B}_{44}\text{N}_6\text{C}_{78}\text{H}_{224}$ (2303.49): C 40.67, H 9.80, N 3.65; found: C 40.68, H 10.10, N 3.80.

[Bu₃NH]₂[Au(SnB₁₁H₁₁)₄] (4): AuCl_3 (120 mg, 0.40 mmol) was dissolved in CH_2Cl_2 (20 mL) and treated with $[\text{Bu}_3\text{NH}]_2[\text{SnB}_{11}\text{H}_{11}]$ (0.99 g, 1.58 mmol) at room temperature. Immediately the color of the solution turned from yellow to red-orange. After the mixture had been stirred for several hours, the solution was washed with water. From the CH_2Cl_2 phase orange crystals of **4** were isolated by slow diffusion of hexane at room temperature. Yield: 0.59 g, 69%. $^{11}\text{B}\{^1\text{H}\}$ NMR (64 MHz, CD_2Cl_2 , 25 °C): $\delta = -15.9$ ppm (br; B2–B11), signal for B12 not detected; elemental analysis calcd (%) for $\text{AuB}_{44}\text{Sn}_4\text{N}_2\text{C}_{60}\text{H}_{184}$ (2136.44): C 33.94, H 8.73, N 3.30; found: C 33.95, H 8.64, N 3.16.

[Bu₃NH]₂[Pt(SnB₁₁H₁₁)₄] (5): The procedure was analogous to that for the preparation of **2**, but $[\text{Bu}_3\text{NH}]_2[\text{SnB}_{11}\text{H}_{11}]$ (1.50 g, 2.41 mmol) and $[(\text{cod})\text{PtCl}_2]$ (0.23 g, 0.61 mmol) were used. Yield of **3**: 0.98 g, 69%; elemental analysis calcd (%) for $\text{PtSn}_4\text{B}_{44}\text{N}_6\text{C}_{72}\text{H}_{212}$ (2308.02): C 37.47, H 9.26, N 3.64; found: C 35.67, H 8.91, N 3.25.

[K[18]crown-6]₆[Pt(SnB₁₁H₁₁)₄] (6): Compound **5** (0.75 g, 0.33 mmol) was dissolved in CH_2Cl_2 (30 mL) and treated with $\text{K}[\text{HBEt}_3]$ (2.00 mL, 1 M in THF). After the gas evolution ceased the mixture was stirred for another hour. The precipitate was isolated by filtration, washed with hexane, and dried under vacuum. The solid was dissolved in $(\text{CH}_3)_2\text{CO}$ (30 mL) and added to a $(\text{CH}_3)_2\text{CO}$ solution of [18]crown-6 (0.60 g). Yellow crystals of $\mathbf{6} \cdot 4(\text{CH}_3)_2\text{CO} \cdot 2\text{H}_2\text{O}$ were obtained at 0 °C. Yield: 0.49 g, 45%; elemental analysis calcd (%) for $\text{PtSn}_4\text{B}_{44}\text{K}_6\text{O}_{36}\text{C}_{72}\text{H}_{188} \cdot 4(\text{CH}_3)_2\text{CO} \cdot 2\text{H}_2\text{O}$ (3278.73): C 30.77, H 6.64; found: C 29.42, H 6.17.

[Bu₃NH]₂[Pd(SnB₁₁H₁₁)₄] (7): The procedure was analogous to that for the preparation of **3**, but $[\text{Bu}_3\text{NH}]_2[\text{SnB}_{11}\text{H}_{11}]$ (2.29 g, 3.69 mmol) and $[(\text{cod})\text{PdCl}_2]$ (0.26 g, 0.91 mmol) were used. Yield: 1.52 g, 75%. Recrystallization was carried out in CH_2Cl_2 by slow diffusion of hexane at 0 °C to give crystals of **7**. Elemental analysis calcd (%) for $\text{PdSn}_4\text{B}_{44}\text{N}_6\text{C}_{72}\text{H}_{212} \cdot 2\text{CH}_2\text{Cl}_2$ (2389.19): C 37.20, H 9.11, N 3.52; found: C 36.98, H 9.47, N 3.41.

[K-dibenzo-18-crown-6]₆[Pd(SnB₁₁H₁₁)₄] (8): Compound **7** (1.52 g, 0.69 mmol) was dissolved in CH_2Cl_2 (40 mL) and treated with $\text{K}[\text{HBEt}_3]$ (4.14 mL, 1 M in THF). After the gas evolution ceased the mixture was stirred for another hour. The precipitate was isolated by filtration, washed with hexane, and dried under vacuum. The solid was dissolved in CH_3CN (30 mL) and added to a solution of dibenzo-[18]crown-6 (1.50 g) in CH_3CN

(10 mL). Yellow crystals of $\mathbf{8} \cdot 4\text{CH}_3\text{CN}$ were obtained at 0 °C. Yield: 1.39 g, 55%; elemental analysis calcd (%) for $\text{PdSn}_4\text{B}_{44}\text{K}_6\text{O}_{36}\text{C}_{120}\text{H}_{188} \cdot 4\text{CH}_3\text{CN}$ (3662.43): C 41.98, H 5.50, N 1.53; found: C 41.53, H 5.96, N 1.53.

[Bu₃MeN]₂(dppp)Pd(SnB₁₁H₁₁)₂] (10): $[\text{Bu}_3\text{MeN}]_6[\text{Pd}(\text{SnB}_{11}\text{H}_{11})_4]$ (**5**) (0.35 g, 0.15 mmol) was treated with 1,3-bis(diphenylphosphino)propane (62 mg, 0.15 mmol) in CH_2Cl_2 (20 mL) at room temperature for 12 h. The color of the solution changed to orange and slow diffusion of hexane into the CH_2Cl_2 layer at 5 °C resulted in the isolation of red crystals of **10** (yield: 70 mg, 36%). ^1H NMR (CD_2Cl_2 , 200 MHz, without signals for $[\text{Bu}_3\text{MeN}]^+$): $\delta = 2.03$ (m, 2H; dppp), 2.33 (m, 4H; dppp), 7.46, 7.78 ppm (m, 20H; Ph); $^{11}\text{B}\{^1\text{H}\}$ NMR (CD_2Cl_2 , 64 MHz, ext. $\text{BF}_3\text{Et}_2\text{O}$): $\delta = -15.6$ (s; B2–B11), -10.0 ppm (s; B12); $^{31}\text{P}\{^1\text{H}\}$ NMR (CD_2Cl_2 , 81 MHz, ext. H_3PO_4): $\delta = 4.9$ ppm (s, $^2J_{\text{P,Sn}} = 2356.4$ Hz); elemental analysis calcd (%) for $\text{PdSn}_2\text{P}_2\text{B}_{22}\text{N}_2\text{C}_{53}\text{H}_{108}$ (1298.34): C 44.92, H 7.68, N 1.98; found: C 44.13, H 7.79, N 2.30.

Acknowledgement

We thank the Deutsche Forschungsgemeinschaft (Schwerpunktprogramm Polyeder) and the Fonds der Chemischen Industrie for financial support. Moreover, we thank Degussa AG for the gifts of chemicals. We also wish to thank PD Dr. A. Möller for assistance with the IR and Raman spectroscopy studies.

- [1] a) W. Petz, *Chem. Rev.* **1986**, *86*, 1019–1047; b) M. S. Holt, W. L. Wilson, J. H. Nelson, *Chem. Rev.* **1989**, *89*, 11–49.
- [2] a) L. A. van der Veen, P. K. Keeven, P. C. J. Kamer, P. W. N. M. van Leeuwen, *J. Chem. Soc. Dalton Trans.* **2000**, *13*, 2105–2112; b) J.-T. Chen, Y.-S. Yeh, C.-S. Yang, F.-Y. Tsai, G.-L. Huang, B.-C. Shu, T.-M. Huang, Y.-S. Chen, G.-H. Lee, M.-C. Cheng, C.-C. Wang, Y. Wang, *Organometallics* **1994**, *13*, 4804–4824; c) I. Tóth, T. Kégl, C. J. Elievier, L. Kollár, *Inorg. Chem.* **1994**, *33*, 5708–5712; d) P. Haelg, G. Consiglio, P. Pino, *Helv. Chim. Acta* **1981**, *64*, 1865–1869; e) J. K. Stille, H. Su, P. Brechot, G. Parrinello, L. S. Hegedus, *Organometallics* **1991**, *10*, 1183–1189; f) I. Tóth, I. Guo, B. E. Hanson, *Organometallics* **1993**, *12*, 848–852; g) A. Scrivanti, V. Beghetto, A. Bastianini, U. Matteoli, G. Menchi, *Organometallics* **1996**, *15*, 4687–4694; h) J. Bakos, S. Cserepi-Szucs, A. Gomory, C. Hegedus, L. Marko, A. Szollosy, *Can. J. Chem.* **2001**, *79*, 725–730.
- [3] C. Y. Hsu, M. Orchin, *J. Am. Chem. Soc.* **1975**, *97*, 3553.
- [4] I. Schwager, J. F. Knifton, *J. Catal.* **1976**, *45*, 256–267.
- [5] a) M. Veith, A. Müller, L. Stahl, M. Nötzel, M. Jarczyk, V. Huch, *Inorg. Chem.* **1996**, *35*, 3848–3855; b) M. Veith in *Metal Clusters in Chemistry* (Ed.: P. Braunstein, L. A. Oro, P. R. Raithby), Wiley-VCH, Weinheim, **1999**, Ch. 1.5, p. 73–90.
- [6] D. J. Cardin in *Metal Clusters in Chemistry* (Ed.: P. Braunstein, L. A. Oro, P. R. Raithby), Wiley-VCH, Weinheim, **1999**, Ch. 1.4, p. 48–72.
- [7] a) M. Contel, K. W. Hellmann, L. H. Gade, *Inorg. Chem.* **1996**, *35*, 3711–3715; b) B. Findeis, M. Contel, L. H. Gade, M. Laguna, M. C. Gimeno, I. J. Scowen, M. McPartlin, *Inorg. Chem.* **1997**, *36*, 2386–2390; c) B. Findeis, L. H. Gade, I. J. Scowen, M. McPartlin, *Inorg. Chem.* **1997**, *36*, 960–961; c) M. Lutz, B. Findeis, M. Haukka, T. A. Pakkanen, L. H. Gade, *Organometallics*, **2001**, *20*, 2505–2509; d) M. Lutz, M. Haukka, T. A. Pakkanen, L. H. Gade, *Organometallics*, **2002**, *21*, 3477–3480; e) L. Gade, *Eur. J. Inorg. Chem.* **2002**, 1257–1268.
- [8] R. W. Chapman, J. G. Kester, K. Folting, W. E. Streib, L. J. Todd, *Inorg. Chem.* **1992**, *31*, 979–983.
- [9] a) T. Marx, L. Wesemann, S. Dehnen, *Organometallics*, **2000**, *19*, 4653–4656; b) T. Marx, L. Wesemann, S. Dehnen, I. Pantenburg, *Chem. Eur. J.* **2001**, *7*, 3025–3032; c) T. Marx, L. Wesemann, S. Dehnen, *Z. Anorg. Allg. Chem.* **2001**, *627*, 1146–1150.
- [10] T. Marx, I. Pantenburg, L. Wesemann, *Organometallics*, **2001**, *20*, 5241–5244.
- [11] L. Wesemann, S. Hagen, T. Marx, I. Pantenburg, M. Nobis, B. DrieBen-Hölscher, *Eur. J. Inorg. Chem.* **2002**, 2261–2265.
- [12] a) J. H. Nelson, N. W. Alcock, *Inorg. Chem.* **1982**, *21*, 1196–1200; b) P. G. Antonov, Y. N. Kukushkin, V. G. Strele, F. K. Egorov, Y. P. Kostikov, *Zh. Obshch. Khim.* **1982**, *52*, 2147–2154.

- [13] A. Albinati, P. S. Pregosin, H. Ruegger, *Angew. Chem.* **1984**, *96*, 63; *Angew. Chem. Int. Ed. Engl.* **1984**, *23*, 78.
- [14] a) D. M. Mingos, H. R. Powell, T. L. Stolberg, *Trans. Met. Chem.* **1992**, *17*, 334–337; b) Z. Demidowicz, R. L. Johnston, J. C. Machell, D. M. P. Mingos, I. D. Williams, *J. Chem. Soc. Dalton Trans.* **1988**, 1751–1756.
- [15] W. Clegg, *Acta Crystallogr. Sect. B* **1978**, *34*, 278–281.
- [16] S. Hagen, I. Pantenburg, F. Weigend, C. Wickleder, L. Wesemann, *Angew. Chem.* **2003**, *115*, 1539–1543.
- [17] X-RED 1.22, Stoe Data Reduction Program (C) **2001** Stoe & Cie GmbH Darmstadt.
- [18] X-Shape 1.06, Crystal Optimisation for Numerical Absorption Correction (C) **1999** STOE & Cie GmbH Darmstadt.
- [19] CCDC-206336 (**2**), CCDC-206337 (**4**), CCDC-206338 (**6**), and CCDC-206339 (**10**) contain the supplementary crystallographic data for this paper. These data can be obtained free of charge via www.ccdc.cam.ac.uk/conts/retrieving.html (or from the Cambridge Crystallographic Data Centre, 12, Union Road, Cambridge CB21EZ, UK; fax: (+44) 1223-336-033; or deposit@ccdc.cam.ac.uk).
- [20] G. M. Sheldrick, SHELXS-97-Program for Structure Analysis, Göttingen, (**1998**).
- [21] G. M. Sheldrick, SHELXL-93-Program for Crystal Structure Refinement, Göttingen (**1993**).
- [22] B. Wrackmeyer, *Ann. Rep. NMR Spectrosc.* **1985**, *16*, 73–186.
- [23] M. J. Mays, P. L. Sears, *J. Chem. Soc. Dalton Trans.* **1974**, 2254–2256.
- [24] J. D. Cotton, P. J. Davidson, M. F. Lappert, J. D. Donaldson, J. Silver, *J. Chem. Soc. Dalton Trans.* **1976**, 2286–2290.
- [25] N. W. Alcock, J. H. Nelson, *J. Chem. Soc. Dalton Trans.* **1982**, 2415–2418.

Received: March 21, 2003 [F4976]